

# THE UTILIZATION OF ERTS - 1 GENERATED IMAGES IN THE EVALUATION OF SOME IRANIAN PLAYAS AS SITES FOR ECONOMIC AND ENGINEERING DEVELOPMENT

By

**E7.5-10203**

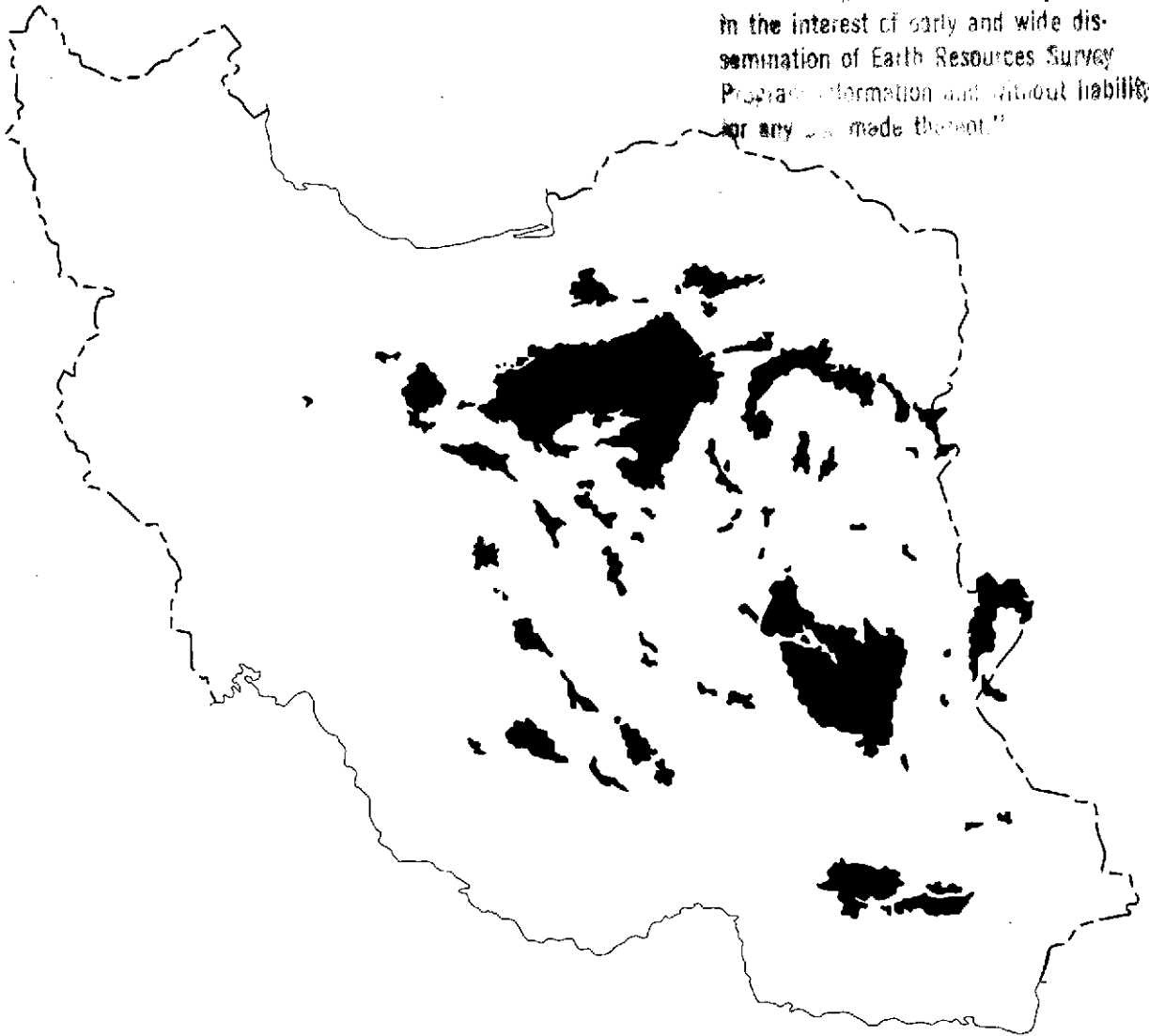
Daniel B. Krinsley

"Made available under NASA sponsorship  
in the interest of early and wide dis-  
semination of Earth Resources Survey  
Program information and without liability  
for any use made thereof."

N75-21728

(E75-10203) THE UTILIZATION OF ERTS-1  
GENERATED IMAGES IN THE EVALUATION OF SOME  
IRANIAN PLAYAS AS SITES FOR ECONOMIC AND  
ENGINEERING DEVELOPMENT, PART 1 Final  
Report, 1 Jul. 1972 - 28 Feb. (Geological

Unclas  
G3/43 00203



## Part I

U.S. Geological Survey  
Reston, Virginia 22092

Final Report—Contract S-70243-AG, MMC # 195A  
Task (30) 434-641-14-03-32  
Prepared For—NASA/Goddard Space Flight Center  
Greenbelt, Maryland 20771

JUNE 1974

TECHNICAL REPORT STANDARD TITLE PAGE

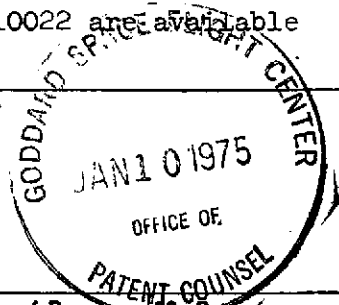
1. Report No.	2. Government Accession No.	3. Recipient's Catalog No.
4. Title and Subtitle THE UTILIZATION OF ERTS-1 GENERATED IMAGES IN THE EVALUATION OF SOME IRANIAN PLAYAS AS SITES FOR ECONOMIC AND ENGINEERING DEVELOPMENT Pt.I (SR 195)		5. Report Date 30 April 1974
		6. Performing Organization Code
7. Author(s) Daniel B. Krinsley (IN 037)		8. Performing Organization Report No.
9. Performing Organization Name and Address Geological Survey National Center (908) 12201 Sunrise Valley Drive Reston, Virginia 22092		10. Work Unit No.
		11. Contract or Grant No. S-70243-AG-3
		13. Type of Report and Period Covered Type III Final Report 1 July 72 - 28 February 74
12. Sponsoring Agency Name and Address Mr. Fred Gordon Goddard Space Flight Center Greenbelt, Maryland 20771		14. Sponsoring Agency Code
15. Supplementary Notes <i>Returned from Patent Office - 1/16/75 sc</i>		
16. Abstract The repetitive coverage of ERTS-1 was used to provide sequential scenes of the Iranian Playas from which hydrologic and morphologic changes were monitored and their economic and engineering significance evaluated, especially on the basis of prior ground control.  At their 1973 maxima, the lakes at Qom and Neriz Playas contained $400 \times 10^6 \text{ m}^3$ and $794 \times 10^6 \text{ m}^3$ of water, respectively. This water, crucial to any agricultural or industrial expansion in these moderately populated areas, should be stored prior to its arrival in the shallow playa lakes where it is annually lost by evaporation.  The Great Kavir in north-central Iran is a vast desert with extensive salt crusts and swamps. During the period of maximum inundation and lowest bearing strengths, as inferred from the image of May 12, 1973, a preliminary road alinement was selected across the Great Kavir. This route avoided the wettest or roughest areas, took advantage of the best terrain, and reduced the road distance between northern and central Iran by as much as 700 km, and the travel time by as much as 10 hours.  Color reproductions of illustrations EDC-010008 to EDC-010022 are available for purchase from the EROS Data Center.		
17. Key Words Suggested by Author Playa Iran Playa lakes Playa roads		18. Distribution Statement 
19. Security Classif. (of this report) Unclassified	20. Security Classif. (of this page) Not applicable	21. No. of Pages Pt. I 48

Figure 2A. Technical Report Standard Title Page. This page provides the data elements required by DoD Form DD-1473, HEW Form OE-6000 (ERIC), and similar forms.

03

III

THE UTILIZATION OF ERTS-1 GENERATED IMAGES  
IN THE EVALUATION OF SOME IRANIAN PLAYAS AS  
SITES FOR ECONOMIC AND ENGINEERING DEVELOPMENT

PRECEDING PAGE BLANK NOT FILMED

Daniel B. Krinsley  
Geological Survey  
National Center (908)  
12201 Sunrise Valley Drive  
Reston, Virginia 22092

30 April 1974

Type III Final Report for Period 1 July 1972 - 28 February 1974

Prepared for:

Goddard Space Flight Center  
Greenbelt, Maryland 20771

1195A

RECEIVED

JAN 03 1975

SIS/902.6

# CONTENTS

## PART I

	Page
INTRODUCTION	1
PHYSICAL SETTING OF THE IRANIAN PLAYAS	3
SURFACE TYPES OF THE IRANIAN PLAYAS AND THEIR CLIMATIC AND GENETIC RELATIONSHIPS	4
PLAYAS INVESTIGATED WITH ERTS-1 IMAGES	6
Qom Watershed	6
Qom Playa	7
Analysis of the ERTS-1 Images of Qom Playa	10
Interpretation of the False-Color Composites	10
Special Graphics by Photographic Techniques	14
Digital Computer Processing and False-Color Compositing	16
Potential for Economic Development	19
Great Kavir Watershed	21
Great Kavir	21
Surface Types within the Great Kavir	23
Potential for Engineering Development	25
Selection of a Preliminary Road Alinement through the Great Kavir	26
Zagros Mountains Watershed	28
Neriz Playa	29
Shiraz Playa	31
Analysis of the ERTS-1 Images of Shiraz and Neriz Playas	33
Potential for Economic Development	36
CONCLUSIONS	37
REFERENCES	40

## PART II

### ILLUSTRATIONS

FIGURES	Page
1. The relationship of playas and associated features to relief in Iran, map.	42
2. Interior watersheds of Iran; playas investigated in this study and the areas of their ERTS-1 images, map.	43
3. Qom Playa, September 4, 1972; false-color composite of ERTS-1 image. EDC-010008.	44
4. Boundary in Qom Playa between the wet muddy area overlain by a thin veneer of salt, and the thick salt crust with raised-ridge polygons, photo.	45
5. Raised-ridge polygons in the salt crust east of Sargardani Island in Qom Playa, photo.	46
6. The single pebble gravel beach along the east shore of Sargardani Island, 1.2 m above the salt crust, photo.	47
7. Lake expansion at Qom Playa, September 22, December 3 and 21, 1972, and May 14, 1973; false-color composites of ERTS-1 images. EDC-010009.	48
8. A comparison of the climatic data from Qom with the lake area at Qom Playa as a percent of the playa area, and the estimated lake volume from September 4, 1972, to May 14, 1973, graphs.	49
9. Composite map of the extent of the lake at Qom Playa on December 3 and 21, 1972, and May 14, 1973. EDC-010010.	50
10. Computer enhanced false-color composite of Qom Playa, September 22, 1972; band ratios 5/6 blue, 5/7 red. EDC-010011.	51
11. Computer enhanced false-color composite of Qom Playa, September 22, 1972; band ratios 5/6, 4/5, 4/6, and 5/7. EDC-010012.	52
12. Computer enhanced false-color composite of Qom Playa, September 22, 1972; band ratios 4/6, 5/7, 5/6, and 4/7. EDC-010013.	53
13. Elements of the Great Kavir, map.	54

FIGURES--Continued

Page

- |     |   |    |
|-----|---|----|
| 14. | Rough black salt ridges and pinnacles adjacent to the dry-season road across the Great Kavir, photo.  | 55 |
| 15. | Existing Iranian roadnet and the proposed Great Kavir road, map.  | 56 |
| 16. | Great Kavir, September 2, 1972; false-color composite of ERTS-1 image. EDC-010014.  | 57 |
| 17. | Great Kavir, September 20, 1972; false-color composite of ERTS-1 image. EDC-010015.   | 58 |
| 18. | Great Kavir, December 19, 1972; false-color composite of ERTS-1 image. EDC-010016.  | 59 |
| 19. | Great Kavir, February 11, 1973; false-color composite of ERTS-1 image. EDC-010017.  | 60 |
| 20. | Great Kavir, March 1, 1973; false-color composite of ERTS-1 image. EDC-010018.  | 61 |
| 21. | Great Kavir, May 12, 1973; false-color composite of ERTS-1 image. EDC-010019.   | 62 |
| 22. | Shiraz and Neriz Playas, May 12, 1973; false-color composite of ERTS-1 image. EDC-010020.   | 63 |
| 23. | Pit in the surficial sediments at Neriz Playa, photo.   | 64 |
| 24. | Collecting salt at the west margin of Shiraz Playa.   | 65 |
| 25. | Lake fluctuations at Shiraz and Neriz Playas, September 2 and 20, 1972, and December 19, 1972; false-color composites of ERTS-1 images. EDC-010021.   | 66 |
| 26. | Lake fluctuations at Shiraz and Neriz Playas, March 1 and 19, 1973, May 12, 1973, and August 28, 1973; false-color composites of ERTS-1 images. EDC-010022.   | 67 |
| 27. | Lake fluctuations at Shiraz and Neriz Playas from September 2, 1972, to August 28, 1973, maps.  | 68 |
| 28. | A comparison of the climatic data from Neriz with the lake areas at Shiraz and Neriz Playas as a percent of the playa areas, and the estimated lake volumes from September 2, 1972, to August 28, 1973, graphs. | 69 |

## TABLES

Page

1. Hydrologic conditions at Qom Playa from September 4, 1972, to May 14, 1973. 70
2. Surficial analysis of Qom Playa on September 22, 1972, from a comparison of regular and computer enhanced false-color composites. 71
3. Hydrologic conditions along critical segments of the dry-season road across the Great Kavir as inferred from ERTS-1 images from September 2, 1972, to May 12, 1973. 72
4. Lacustrine fluctuations at Shiraz and Neriz Playas from September 2, 1972, to August 28, 1973, as inferred from ERTS-1 images. 73

## INTRODUCTION

Playas are almost flat landforms whose surfaces were in most cases covered by Pleistocene lakes. Composed of relatively homogenous materials and characterized by a general lack of relief or of vegetation, their micro-relief changes with fluctuations in the level of ground water. Playas are common features of the arid regions landscape and consequently they have widespread global distribution.

Iranian playas occupy only 6 percent of the land area of Iran, but most of the population lives adjacent to the margins of the playas because of the availability of flat land and moderate supplies of ground water at relatively shallow depths. The playas are potentially valuable sources of water and chemicals, and could be utilized for the emplacement of roads and inexpensive airfields or as agricultural areas. The playas have not been fully utilized to date because of the lack of adequate knowledge concerning the seasonal changes in their surface and ground water hydrologies and in the physical properties of their sediments. Most playa investigations have been conducted during the summer when the surficial sediments are dry and have sufficiently high bearing strengths to support men and vehicles. Because of seasonal changes in their hydrology and consequently in the characteristics of their sediments, playas are dynamic landforms which are continually and significantly changing.

Sixty playas within the interior of Iran (fig. 1) have been studied since 1965 (Krinsley, 1968, 1969, 1970, 1972a, and 1972b). These ranged in area from 25 to 52,825 km<sup>2</sup> (Great Kavir). Thirty-three playas are smaller than 300 km<sup>2</sup>; except for the Great Kavir, the largest playa is



4,685 km<sup>2</sup>. Twenty-two playas were investigated on the ground, 20 were observed from low-flying aircraft, and 18 were viewed solely from aerial photographs and from ERTS-1 multispectral scanner (MSS) images.

The repetitive coverage of ERTS-1 is ideally suited to provide seasonal images of the Iranian playas from which changes in the areal extent and morphology of the surficial materials may be recorded in conjunction with contemporaneous or previous ground truth studies of actual surficial conditions. Data derived from the analyses of ERTS-1 images can provide a rational basis for planning the economic utilization (salts or water extraction and agriculture) and engineering development (roads and airfields) of these playas.

ERTS-1 images used in this study have been examined in single bands and in false-color composites of several band combinations. Enhancement techniques combining digital computer processing with false-color compositing are also employed. Sequential hydrologic changes in a playa are graphically illustrated by using a new three-stage masking process. The potential use of the ERTS-1 system and the rapidly evolving methodologies for that use are discussed in this report.

#### NOTE

Illustrations originally in color are identified in their caption by an EDC-0100\_ number. Copies of the original color are available for purchase from the EROS Data Center, Sioux Falls, South Dakota 57198, using the EDC number. Prices are available on request.

## PHYSICAL SETTING OF THE IRANIAN PLAYAS

The playas of Iran are widespread in the interior lowlands, but also occupy many intermontane basins. The principal components of the environment that shape and influence the playas are lithology and structure, relief, drainage, climate, and vegetation.

The Elburz and Zagros Mountains were compressed against the relatively older inflexible block of the Iranian Plateau to the east during the Plio-Pleistocene phase of the Alpine Orogeny. Lower, but nevertheless rugged mountains that formed along Iran's eastern border divide the plateau into an eastern basin in Afghanistan and western basin in Iran. Within the western basin are several lesser mountain chains and isolated mountains as well as extensive desert plains. The lowest depressions in these deserts are occupied by the playas (fig. 1).

Approximately half of Iran consists of basins from which there are no outlets and from which the collected drainage is removed by evaporation. Moist winds bring considerable precipitation during the winter half of the year to the northern slopes of the Elburz Mountains which effectively bar movement of moisture to the south. Similarly, the Zagros Mountains act as a barrier to the moisture-laden westerlies. Rainfall is quickly reduced in amount southward and eastward so that the interior lies within a vast rain shadow, and becomes increasingly arid from west to east and from the north to south. There is exterior drainage only along the north, west, and south margins of the country; the remainder has interior drainage.

There is a considerable water deficit in the interior during all seasons, and streams that do reach the playas are generally fed by ground

water. The upper aquifers in the alluvial fans are phreatic, but towards the center of the basin artesian conditions develop as a result of confining clay layers (Issar, 1969, p. 94). The uppermost aquifer does remain phreatic to the margin of the playa, where the water from the toe of the fan spills out over the playa surface creating a "wet zone." Evaporation through the capillary zone from the phreatic aquifer results in salinization of the water. Salinization is accentuated in the north-central basins that are underlain by Miocene evaporites.

Although man has severely altered the natural vegetation by extensive cutting, it is doubtful that vegetation within the inner plateau seriously affected the amount and intensity of overland flow during the Pleistocene. It seems more likely that increased cold during the glacial periods more than counteracted any relative increase in humidity that might have been favorable to growth. Significantly, no evidence has been found in any of the upper Pleistocene sediments, along the inner mountain flanks or in the playas, of buried trees or other vegetative debris.

#### SURFACE TYPES OF THE IRANIAN PLAYAS AND THEIR CLIMATIC AND GENETIC RELATIONSHIPS

Surficial types recognized within the playa areas consist of fan deltas, wet zones, clay flats, salt crusts, intermittent lakes, perennial lakes, and swamps (Krinsley, 1970, p. 262). The condition, extent and areal distribution of these surficial types have great climatic and genetic significance.

Prominent fan deltas are located at the termini of former large, probably perennial streams which headed in the Elburz or Zagros Mountains.

The size of the fan deltas in relation to the present stream load and regimen indicates that these features are relicts of streams with considerably greater discharge. No prominent fan deltas were observed in the more interior watersheds. Wet zones are almost entirely located within an irregular band which can be followed clockwise from Iranshahr in the southeast to the Eastern Mountains. Wet zones are generally absent or poorly developed in the southeastern playas, which is a reflection of the aridity in that part of Iran. A recent expansion of the wet zones at the expense of other drier surface types suggests a rising water table as the result of increased runoff. Clay flats are found in almost all the watersheds; where they are absent, there are well-developed wet zones. The clay flat predominates in the northeastern and south-central watersheds, probably because of the general absence of Miocene evaporites which produce salt crusts, and the absence of water to form wet zones. The clay flat is the predominant type of playa surface formed during the recent past.

Distribution of the salt crusts is correlated not only with proximity to the Miocene rocks but with a high local water table. Consequently, the playas of open basins, even those underlain by Miocene evaporites, may contain only clay flats. As indicated, the salt crusts are mainly derived from the weathering and erosion of the Miocene evaporites rather than from concentration in deep lakes of salts leached from low-saline rocks over a long period of time (as for example, in Lake Bonneville and Lahontan of the western United States). If the latter case applied in Iran, there would be evidence of high beach lines and fractional crystallization of the salts. Instead, the salt crusts have grown as a

result of the accretion of thin salt layers from the evaporation of briny water that periodically floods the playa surface and which comes from the area of the Miocene rocks. The salt crusts are currently expanding, apparently in continuation of a long uninterrupted trend in recent history.

Strand-lines and beaches at four of the six intermittent lakes indicate that they were the sites of somewhat larger, deeper permanent lakes in the past, which were, however, shallow in comparison with Lake Bonneville. The only permanent lake of significant size, at present, in the interior drainage region is the Hamun-i-Helmand at Zabol near the Afghanistan border. This lake owes its existence primarily to the Helmand River which heads in Afghanistan. Swamps occur around the margin of the Hamun-i-Helmand and in the playa west of Iranshahr. These swamps are fed by streams with reduced but generally dependable flows during the dry season.

#### PLAYAS INVESTIGATED WITH ERTS-1 IMAGES

Playas investigated in this study lie in the Qom, Great Kavir and Zagros Mountains Watersheds of Iran (fig. 2). The playas were selected on the basis of their potential for economic development and on the availability of good seasonal ERTS-1 coverage.

#### Qom Watershed

The Qom Watershed lies in a corridor approximately 300 km wide between the southwest flank of the Elburz Mountains and the northeast flank of the Zagros Mountains (figs. 1, 2). The highest altitudes are

north of Tehran but decrease northwestward along the divide with the exterior drainage region. The divide ridge rises again along the southeastern and northeastern divides of the watershed.

Igneous rocks are responsible for most of the positive relief in the watershed, except for the southwestern divide which contains slates, shales, sandstones, and some coal beds, and the northwestern divide composed of folded Plio-Pleistocene coarse clastics. Miocene evaporites are widespread in the lowlands. They provide the channelways for the principal streams and are the source for the playa salt crusts.

The 300 mm isohyet lies close to the northeast divide, and extends further into the watershed near the northwest and southwest divides. Greater precipitation from the west is reflected in the drainage pattern which is best developed along the west and southwest divides.

#### Qom Playa

Qom Playa occupies the easternmost and lowest part of the watershed (765 m). Igneous and evaporitic rocks comprise most of the northeast and southeast ridges adjacent to the playa and a large dune field borders its southern margin. The northwest margin adjoins extensive alluvial plains whose streams mostly originate in the Zagros Mountains. The playa has the general form of an equilateral triangle with sides approximately 60 km long (fig. 3).

Qom Playa receives discharge along its western margin (fig. 3) from three streams that head in the Zagros Mountains: the Qara Chai, Rud-I-Shur, and Qom Rud. The largest, the Qara Chai, has maximum flow of 308 m<sup>3</sup>/sec in the spring, and a minimum in October of 4 m<sup>3</sup>/sec

(Oberlander, 1968, p. 271). Qom Playa is annually inundated at its northwest part by shallow water which occasionally spreads over the entire playa surface. This water generally evaporates by mid-September leaving a wet muddy area overlain by a veneer of salt (fig. 4).

A thick salt crust, which covers two-thirds of the playa (figs. 3, 4) gradually thins towards this wet area (Huber, 1960). The salt crust is sharply delineated by polygons ranging from one to 6 m in diameter with ridges generally 6 to 20 cm high, respectively (fig. 5). A section of salt crust 6.8 m thick immediately north of Sargardani Island, adjacent to the south coast (fig. 3), shows no significant unconformities. This crust is underlain by four other salt horizons separated by beds of clay and silt, all of which are underlain by a thick, practically salt-free lower deposit of clay with some sand (Krinsley, 1970, pl. 1). This sequence suggests that the depositional environment of this playa has alternated from conditions of high evaporation and low runoff (salt crust formation) such as currently prevail, to conditions of lower evaporation and higher runoff forming water surpluses that resulted in lakes and consequently in lacustrine sediments (Huber, 1960). Other playas of this type as well as other salt-crusted playas probably contain similar sequences of sediments.

Several islands project through the salt crust near the south shore of the playa. The largest of these, Sargardani Island (figs. 3, 5), rises 70 m above the playa. Approximately 20 percent of the island consists of hills and ridges with flat to rounded summits bounded by 30° to 35° gullied slopes. These are cut at their base by pediments (fig. 5). The pediments are generally mantled by alluvial fans, but scattered inselbergs

indicate that the rock surface is at shallow depth. The slope of the fans decreases from 4° at the toe of the hill-slope to 2° at their line of truncation by a beachline (fig. 5). Bedrock on the island is composed of rhyolite which weathers into a reddish yellow (7.5 YR 6/6) soil. The flat to rounded summits are armored with a pavement of coarse, angular gravel which is pitted by sand abrasion. Beneath the gravel, a zone of weathered rhyolite with 14 percent clay is locally 30 cm deep and grades into bedrock.

A single beach cuts the fans around Sargardani Island 1.2 m above the salt surface (fig. 6). Neighboring islands are similarly bordered by a 1-2 m beach. There are no beaches nor beach remnants thus far reported around the perimeter of Qom Playa and none were seen during an aerial reconnaissance around the shore of the playa in August, 1967. These observations suggest that the islands may occupy a depression in the playa surface.

An extensive dune field (erg) south of Qom Playa consists of great overlapping sheets of sand which resemble shingles overlapping to the southeast. Although the erg is large (693 km<sup>2</sup>), it is not possible to ascribe this deposit exclusively to a glacial period because the dunes are currently very active. The source of the sand is the large alluvial plain between Qom and the playa (figs. 2, 3).

Qom Playa originated as a tectonic basin, but in the absence of any faulting immediately adjacent to or within the playa sediments, it must be assumed that it has not been subsequently disturbed. Filling of the basin continued perhaps throughout the entire Pleistocene. Sediments have moved over long pediments where attrition has reduced particle size.



The materials were possibly deposited in a shallow lake during cool periods of low evaporation. Arid periods were times of salt encrustation. This genesis conforms with the playa stratigraphy, slope of the subsurface margin, and the absence of any beaches around the playa. The preservation of the single beach around Sargardani Island is due to its recency and the absence of a concentrated drainage.

The morphologic and stratigraphic evidence from the Qom Watershed indicates that previous periods of erosion and deposition may have been significantly different than those which are operative today. These "indicators" suggest previous climates that were alternately cooler and perhaps more moist, and then warm and dry as at present.

#### Analysis of the ERTS-1 Images of Qom Playa

The basis for the analyses of the ERTS-1 images of Qom Playa and of the other playas in this study is familiarity with actual ground conditions and sediments at these playas during the summer and autumn of 1965, 1966, 1967, and 1972. In addition to ground control, these playas were viewed from low-flying aircraft, and many of their details were compiled from aerial photos at a scale of 1:30,000 and 1:60,000.

#### Interpretation of the False-Color Composites

Initially, false color diazo transparencies were prepared from positives of ERTS-1 images. Yellow, red, and blue were used for bands 4, 5, and 7 respectively. These three colors were then composited to form a false-color transparency. The composite was then compared to actual ground and aerial photos and interpreted in the light of the

investigator's experience. The false-color illustrations used in this report are products of a subtractive color system. The dyes used in this system are magenta, yellow, and cyan, but the resultant pure colors are red, green, and blue. False-color composites of Qom Playa were prepared from the ERTS-1 positives of six scenes (figs. 3, 7). These are identified in table 1 which summarizes the hydrologic conditions in the playa from September 4, 1972, to May 14, 1973. These data were obtained by measuring the areas of the lake, wet zone and salt crust in each scene.

In the false-color composites, water is blue, salt is white, and silt and clay have a reddish-brown color. The purity or intensity of these colors reflect differences in the composition, hydrology, or morphology of the surface materials. With increasing depth, water ranges in color from aquamarine to dark blue to black (fig. 7). With increasing saturation, the salt crust ranges in color from pure white to aquamarine. With increasing roughness or microrelief the salt crust ranges in color from pure white (smooth crust) to yellow-white (rough salt crust or salt crust with raised-ridge polygons). With increasing silt and clay load, the streams, playa lake currents and salt crust surfaces range in color from pink to reddish brown (fig. 7, December 21, 1972). Combinations of wet, silty and rough salt crust result in mixed false colors which require special consideration in their correct interpretation. Because of its more immediate economic importance, emphasis has been placed on the development and extent of the playa lake.

On September 4, 1972 (fig. 3), the lake occupied 3 percent of the playa area and had an estimated average depth of 0.5 m and an estimated

volume of  $33 \times 10^6 \text{ m}^3$  (fig. 8). The estimated average depth of the lake at this time is based on the intensity of the blue color and on comparable playa lakes such as those in the Zagros Mountains Watershed, which also have very low subsurface gradients and which have been measured near the times of their annual high stands (see page 30). The water was clear indicating a previous period of sediment settlement and quiescence. The wet area contained 20 percent of the playa area, and the locally moist salt crust occupied 77 percent of the playa area (table 1).

The lake had evaporated by September 22, 1972 (fig. 7), leaving a thin veneer of salt. The wet area, including the area previously occupied by the lake, increased to 23 percent of the playa area; and the salt crust area, now dried out, remained constant at 77 percent. This period at the end of the long, hot summer, during which rain is generally absent (fig. 8) and evaporation rates are highest, has the lowest ground water levels of the year.

A lake reoccupied 7 percent of the playa area by December 3, 1972 (fig. 7). It had an estimated average depth of 0.5 m and an estimated volume of  $65 \times 10^6 \text{ m}^3$  (fig. 8). No ERTS-1 images were available for October and November of 1972, but the climatic data suggest that the lake may have been very close to its December 3, 1972, stage by late-October rather than by mid-November as indicated on the graph. Light brown tinting in the water indicates a light sediment load and suggests recent influx. The wet area (17 percent) was diminished by the area of the lake, and the salt crust area was almost constant (76 percent). Light reddish staining diminishing in intensity northward from the southern perimeter of the playa suggests a recent influx of silt and clay-laden water from streams entering the playa along its south border.

There was a dramatic increase in the size of the lake (18 percent of the playa area) by December 21, 1972 (fig. 7). In view of the only moderate increase in precipitation during December (fig. 8), it is reasonable to assume that there had been sufficient ground water recharge during October and November so that the December runoff quickly accumulated on the surface of the playa. The average depth of the lake is conservatively estimated to have been 1.0 m, and its volume at least  $342 \times 10^6 \text{ m}^3$ . The lake occupied the northern half of the wet area, the lowest part of the playa, and reduced that area to 12 percent of the playa. Dark-brown tinting of the water indicates a heavy sediment load with the recent and continuing influx. The wet area, south of the lake, contained scattered shallow ponds and sediment stains. The salt crust area slightly reduced to 70 percent of the playa area was heavily stained by sediment laden streams from the southern perimeter of the playa. The lake area increased to 19 percent of the playa by January 8, 1973. This scene is partly obscured by clouds and is not illustrated. The average depth of the lake is estimated to have been 1.0 m and the volume  $364 \times 10^6 \text{ m}^3$  (fig. 8). This period, the coldest part of the year with the lowest evaporation rates, is a time for maximum water accumulation. Note that there was an estimated increase in the volume of the lake of  $22 \times 10^6 \text{ m}^3$ , although January and December have the same mean monthly precipitation totals. Sediment staining in the lake had diminished suggesting that the principal period of influx had terminated. The wet area increased slightly to 15 percent at the expense of the salt crust (to 66 percent). Staining is diminished but was continuing in the wet area and over the salt crust near the southern perimeter of the playa.

Although there are no ERTS-1 scenes of Qom Playa for June 1973; the climatic data suggest that the lake reached its maximum extent at approximately the time of the May 14, 1973, scene (fig. 7). The lake then occupied 21 percent of the playa with an estimated average depth of 1.0 m and an estimated volume of  $397 \times 10^6 \text{ m}^3$  (fig. 8). Light, reddish tinting of thin lake currents suggests greatly diminished influx. The wet area (13 percent) has local, scattered ponding, and the salt crust area (66 percent) is saturated in 2/3 of its area, with local ponding and light silt staining.

#### Special Graphics by Photographic Techniques

A three-stage masking technique, developed by Mr. Joseph McSweeney of the U. S. Geological Survey, was employed in the construction of a false-color diazo composite map of the hydrologic changes that occurred in Qom Playa from September 22, 1972, to May 14, 1973 (fig. 9E). For each of the initial three scenes in which the lake appears (fig. 9A, B, C), a black-and-white negative was prepared from the ERTS-1 MSS, 9.5 inch positive transparency of band 7. The negative of band 7 then was combined with the positive transparency of band 4 from that same scene to form a sandwich; and, a positive transparency was made from this sandwich. A false-color diazo was made from each of these positive transparencies (fig. 9A, B, C). These false-color diazo were combined and superposed on a simple false-color diazo composite made from positive transparencies of band 5 and band 7 of the September 22, 1972, scene (fig. 9D).

In order to accentuate the hydrologic changes that occurred, and to compensate for the effects of additive colors, scenes A, B, and C (fig. 9)

were printed in red, blue, and yellow, respectively. The simple false-color composite of the September 22, 1972, base stage, with no lake (fig. 9D), consists of band 5 (red) and band 7 (blue).

There are two difficulties with this technique which require some care. Because of the satellite drift between scenes of the same area, registration cannot be made to the usual peripheral cross-hairs, but must be made to prominent landmarks. In the case of figure 9, registration was made to the playa outline and to Sargardani Island. Another problem is the use of colors in the false-color composites, which should remain distinctive and yet not interfere with each other. In figure 9D, blue in the base is very weak in the September 22, 1972, scene and does not interfere with its use in the December 21, 1972, stage. Blue on yellow becomes green which is distinctive in the map. Yellow (band 4) is eliminated from the base stage (September 22, 1972) because it would interfere with the May 14, 1973, scene (yellow); its absence diminishes the delineation of the dry salt crust, but this is not important to the purpose of this map.

An additional map illustrating and accentuating the increase in sediment load during the period December 7, 1972, to December 21, 1972, is in preparation. Band 5 which is most sensitive to sediment load, is utilized in the preparation of the black-and-white negative and positive transparency (band 4) sandwich. With ground control measurement of sediment load at critical periods, correlated with contemporaneous satellite images, it would be feasible to monitor sediment load by satellite.

## Digital Computer Processing and False-Color Compositing

This technique which combines digital computer processing with false-color compositing was developed in order to enhance subtle spectral reflectivity differences among natural materials (Billingsley and Goetz, 1970). Recent applications of this technique to rocks and minerals are detailed in a study by Rowan, Wetlaufer, Goetz, Billingsley, and Stewart (in preparation). Image enhancement is accomplished in a computer by ratioing the digital numbers of two MSS bands, contrast stretching the resultant ratio values, and generating a new black-and-white ratio image which shows reflectance differences. Radiance variation due to albedo and topography are minimized through the ratio processing. Geometric corrections are also made to compensate for distortions caused by the earth's rotation relative to the satellite's movement. Contrast stretching increases the contrast in areas of the image that have generally uniform albedos. In Qom Playa, for instance, the wet area was stretched in order to accentuate subtle differences in the composition and hydrology of the generally light-colored surficial materials with no relief. This is also the area of more immediate economic importance.

Additional enhancement is achieved by preparing false-color diazo composites made from positive transparencies of the stretched-ratioed images. Geometrically corrected, stretched-ratioed images of the September 22, 1972, scene of Qom Playa were prepared at the Jet Propulsion Laboratory. Diazo color transparencies were made from positive transparencies of these images, and the former were combined as false-color diazo composites.

Positive transparencies of six stretched-ratioed images (bands 4/5, 4/6, 4/7, 5/6, 5/7, 6/7) were each prepared in four colors (blue, red, yellow, and green), and experimentally combined in composites of two to four color-ratios. Approximately 30 color-ratio composites were prepared of which 3 were selected that best illustrate the enhancement potential of this technique.

In order to interpret correctly the color-ratio composites, they were compared to the standard false-color composite with MSS bands 4, 5, 7 (yellow, red, and blue) for September 22, 1972 (fig. 7, table 2). The combination of MSS band ratios 5/6 blue and 5/7 red (fig. 10, table 2) provides great contrast between the wet area and the dry salt crust. Darkest central and peripheral zones of the wet area are smooth white salt that has been recently precipitated or washed. Purple areas contain wet salt, and the pink annular zone around the wet area is most probably very shallow or ponded water. The magenta area is salt crust with raised-ridge polygons (fig. 5). Small scattered violet areas in the northern half are smooth salt crust probably washed during the previous wet season when they contained some shallow standing water. Sargardani Island is faintly outlined, but the island in the eastern corner of the playa is not visible (figs. 7, 10).

The combination of MSS band ratios 5/6 blue, 4/5 red, 4/6 yellow, and 5/7 green (fig. 11) provides great contrast between the wet and dry salt areas, and good contrast between the elements of the wet and dry salt areas. Green central and peripheral zones of the wet area are smooth white salt that has been recently precipitated or washed during seasonal flooding. Blue areas contain wet salt, and the orange to white



annular zone around the wet area is most likely very shallow or ponded water. The brown area is salt crust with raised-ridge polygons. Small scattered green areas in the northern half are smooth salt crust probably washed during the previous wet season. Sargardani Island and the small island in the eastern corner of the playa are light green (figs. 7, 11). The white-green area at the south shore is probably wet smooth salt crust with admixed clay and silt.

The combination of MSS band ratios 4/6 blue, 5/7 red, 5/6 yellow, and 4/7 green (fig. 12) provides excellent contrast between the two main playa areas and between the zones within these areas. Brown central and peripheral zones of the wet area are smooth white salt recently precipitated or washed. Yellow zones are wet and greenish-yellow locations may be films of water, especially in the south-central part of the wet area. The light blue annular zone around the playa is most likely ponded water. The blue to brown area is salt crust with raised-ridge polygons. The dark-blue to brown zone is stained by silt and clay carried onto the salt crust by water originating at the south shore of the playa during the previous wet season (see fig. 7, September 22, 1972). Small scattered light brown zones in the northern half are smooth salt crust probably washed during the previous wet season, but not stained. The islands are outlined (figs. 7, 12) and the very light brown area at the south shore is probably wet smooth salt with some admixed clay and silt.

The salt crust adjacent to the east shore of Sargardani Island (fig. 5) contains 90 percent salt (halite and gypsum), 6 percent clay (chlorite, kaolinite, and illite), and 4 percent feldspar and quartz. No other salt samples are available at this time. Although most of the

colored zones of the dry salt crust, in the computer enhanced composites, can be interpreted in terms of hydrologic or morphologic conditions within a generally uniform lithology, tonal or subtle color differences that are present locally may reflect different salt minerals. It would be most valuable to field check sites at Qom Playa with specific color differences on the enhanced composites that may be independent of hydrologic or morphologic differences in the salt crust. Conversely, known playa sites with different salt minerals should be analyzed by computer-enhanced ERTS-1 images to pursue the possibility that even subtle differences in spectral reflectivity can delineate minerals or mineral assemblages of economic value.

False-color composites of Qom Playa containing bands 4, 5, and 7 (yellow, red, and blue, respectively) approach reality with respect to earth materials and water, and permit a generalized surficial geologic and hydrologic analysis. False-color-ratio composites in certain combinations both accentuate and delineate subtle differences in spectral reflectivity that are easily ignored or are not visible in the simple false-color composites of Qom Playa. Contrast between areas and within zones (table 2) is much sharper and color differences highlight these distinctions.

#### Potential for Economic Development

Qom Playa, in west-central Iran, is the sump for a drainage basin of 86,812 km<sup>2</sup>, and lies adjacent to the city of Qom and its extensive farmlands and oil resources.

During the period from September 4, 1972, to May 14, 1973, Qom Playa was driest from mid-September to late-September (figs. 3, 7). The playa was almost completely saturated by mid-May (fig. 7). The period of greatest lake fluctuation occurred in mid-December when the lake area almost tripled, and the lake volume increased more than five times (fig. 8). At or near its 1973 maximum extent, the lake is conservatively estimated to have contained approximately  $400 \times 10^6 \text{ m}^3$  of water. This enormous resource is annually lost to evaporation.

Diversion, storage, and utilization of this water is facilitated by the geographic location of the source, and the settlement patterns around the playa. The lake's three principal streams form a composite alluvial plain that borders the western margins of the playa (fig. 3). The city of Qom and its hinterland receive their water from these streams, wells, and qanats of this huge alluvial plain. There is almost no settlement along the northern, eastern, or southern margins of the playa. Small earthen dams in the plains and larger dams upstream could store the water during the period of maximum discharge (fig. 8) and extend its use during the summer dry period. There would be little or no negative economic effect of the lowered ground water table east of the alluvial plains. In fact, the depressed water table of the playa would result in a firm hard crust throughout the year which would facilitate transportation, and exploration for salts of economic value. The juxtaposition of the agricultural and oil resources of the Qom area, possible salts of economic value in the playa, and significantly increased utilization of the available supply of water are natural advantages for economic development that should be more thoroughly investigated and considered.

## Great Kavir Watershed

The Great Kavir Watershed (fig. 2) occupies an area of 200,747 km<sup>2</sup> in the northeastern quadrant of Iran. The northwestern divide, in the Elburz Mountains, has summit altitudes which decrease from 4,002 m in the west to about 3,000 m in the east. The southwestern and southeastern divides have summit altitudes which generally range from 1,500 to 2,000 m with a few peaks just under 2,400 m along the southeastern divide. Within the watershed the lowest altitudes are found at the surface of the salt crust basins, and the lowest of these lies at an altitude of 650 m.

### Great Kavir

The central and lowest area of the Great Kavir Watershed is occupied by the Great Kavir, a desert area of 52,800 km<sup>2</sup> (fig. 13). In Iran, the term "kavir" is a generic name for playa. The Great Kavir contains numerous depressions occupied by true kavirs which have imparted their character to the entire desert.

The annual precipitation decreases from a maximum of 300 mm near the divide, but within the rain shadow of the Elburz Mountains, to less than 100 mm in the Great Kavir. Mountains along the northeast divide benefit from moisture-laden air skirting the southern shore of the Caspian and penetrating the valleys and lower passes northeast of Damghan (fig. 1). Precipitation in this eastern area ranges from 100 to 150 mm in the mountains, but there is considerably less in the adjacent lowlands.

In spite of the rapid decrease in precipitation southward, broad valleys with underfit and intermittent streams, below the mountain front,

attest to the past erosional effectiveness of the southward flowing streams. Coarse alluvium including gravel beds, which are interbedded with clay, extends further into the basin with increasing depths in the section. This stratigraphic relationship suggests previously greater stream discharges capable of transporting coarser materials further from their source.

The surface of the Great Kavir ranges in altitude from 850 m in the northwestern part to 650 m near the northeastern boundary. It is underlain by Miocene rocks of the Upper Red Formation (Gansser, 1955, p. 291). These intricately folded siltstones, marls, anhydrites, and salt beds have been eroded to a peneplain where they are exposed over an area of 19,300 square kilometers.

The Great Kavir may be subdivided into eastern and western basins separated by the uplifted peneplain cut into the Miocene rocks. Three central areas of salt crust in a north-south alignment (fig. 13) approximate the peneplain divide. The location of this divide near the western boundary of the peneplain, and the development of two east- to northeast-trending troughs (occupied by linear wet zones) in the eastern half of the peneplain indicate that the regional slope has long been toward the east. It is likely that currently active streams flowing westward into the western basin will eventually breach the divide by headward cutting and shift the divide eastward. The present stream cutting is due to increased gradients resulting from recent tectonism. The Miocene rocks and the younger sediments are cut by currently active northeast-trending faults, the principal one of which is the Great Kavir Fault (fig. 13).

## Surface Types within the Great Kavir

The surface types within the Great Kavir are the Miocene rocks, locally pierced by salt domes, dune fields, fan deltas, wet zones, clay flats, and salt crusts. The areas occupied by these surface types have been generalized at a scale of 1:2,500,000 and then reduced in figure 13. Small areas of these types which appear in ERTS-1 images (scale 1:1,000,000) may not be shown in figure 13.

Miocene rocks consisting of evaporites and other generally saliferous sediments occupy 35 percent of the area of the Great Kavir. At the peneplained surface of these rocks is a thin regolith of clay, silt, and sand with up to 47 percent halite. As a consequence of repeated dissolution of the salt in winter rains and crystallization upon the evaporation of surface moisture, or the summer evaporation of capillary water, the regolith has been churned into a rough surface resembling a plowed field. Across this vast almost flat surface, narrow drainageways terminate in the wet zones or salt crusts. Salt domes, which have locally pierced the Miocene rocks, are similarly cut by the peneplain.

The dune fields occupy 13 percent of the Great Kavir and are situated along its southern and southeastern borders. Fan deltas are large alluvial fans which transgress other surface types. The toes may be completely inundated during the principal runoff period, with the result that peripheral deposition occurs in water, as at a delta. The two large fan deltas in the Great Kavir occupy 5 percent of its area.

The wet zone is a transitional zone which is periodically inundated and always wet. It commonly borders the toes of alluvial fans and fan

deltas, but it also occupies linear basins or narrow troughs within the area immediately underlain by Miocene rocks. The linear wet zones have surface gradients of less than one degree, sloping toward the salt crust areas. Wet zones constitute 4 percent of the Kavir surface. The clay flat, which occupies only 2 percent of the area of the Kavir, is a generally firm surface underlain by dry clay and silt, with variable amounts of salt. It is distinguished from the wet zone, with which it is pedologically identical, on the basis of its higher position above the dry-season water table. The salt crust occupies 41 percent of the Kavir surface in basins in the east, center, and west. The eastern basins are generally continuous, but are locally interrupted by Miocene outcrops in the form of northeast-trending ridges. The surface of the southern basin in the eastern area is 50 m higher than the northern salt surface adjacent to the fan delta. There is thus significant gradient northward toward the fan delta. Three salt-crust basins in the central area of the Kavir occupy downwarps in the Miocene rocks. The salt crusts of these basins lie at different levels, and they are probably hydrologically independent. The larger middle basin surface is estimated to be at an altitude of approximately 850 m.

In areas of thick, white salt crusts and seasonally high water tables, the wet briny muds beneath the crusts may be more thermally expanded than the crusts. This process is facilitated by the transparency of pure salt to infrared rays and by the heat absorption of the black mud. Occasionally, the plastic muds are forced from beneath the salt plates outward and upward through the peripheral cracks. Rapid evaporation of the mud brines results in the formation of black salt dikes along the polygonal cracks (fig. 5).

Grooves and scratches preserved in the solidified dike, that were cut by pre-existing crystallized salt during extrusion of the mud, attest to the rapidity of the solidification.

The uneven extrusion of the briny mud frequently results in the tilting of the polygonal salt plates. Eventually, the area becomes a rough, jumbled mass of sharp and angular black salt blocks with ridges and pinnacles (fig. 14). Wind-driven rain and silt tend to modify and sharpen the rough surface features of these salt fields. Aeolian or alluvial silt added to the old salt, already darkened by the admixed black mud from beneath the crust, imparts a dark matte appearance to this grotesque surface. Relief among the salt pinnacles and ridges ranges from 30 to 50 cm.

Salt crusts and related surface features are primarily a reflection of the hydrologic regime within a basin. The crusts tend to buckle when they are thin, darkened by silt and underlain by light-colored sediments and a seasonally depressed water table. Saline muds are more likely to be extruded when they are black, and water saturated, beneath a relatively thick, white salt crust.

#### Potential for Engineering Development

Almost all materials produced in northern and central Iran are exchanged by means of trucks moving along the east-west and northwest-southeast road that passes through Tehran (fig. 15). Goods from the north destined for the region immediately south of the Great Kavir must travel more than 900 km rather than the 200 km that would be required if an all-weather road existed across the desert. Less dramatic but nevertheless



significant savings in time and in transportation costs could be achieved with such an all-weather road terminating at Nain farther to the southeast (fig. 15). Trucks traveling from Damghan to Nain cover the 750 km in 9 hours; the route across the Great Kavir would be 450 km and require 6 hours.

Rough dry-season roads of gravel and dirt exist for caravans or 4-wheel drive vehicles along the route indicated in figure 15, between Damghan and Nain. Engineering procedures associated with paved-road construction in mountainous areas would be required to complete the segments of the route north and south of the Great Kavir. Engineering procedures associated with the construction of an all-weather road across the Great Kavir would be concerned with stabilizing, strengthening, or constructing a subgrade over the saliferous surficial materials, and installing culverts and bridges to permit normal drainage across the route of the eventual road alignment. This section of the report is concerned with the use of ERTS-1 scenes in the selection of a preliminary road alignment through the Great Kavir.

#### Selection of a Preliminary Road Alignment through the Great Kavir

The area of the Great Kavir most suitable for the construction of an all-weather road lies entirely within one ERTS-1 scene (figs. 2, 16). The center point of the September 2, 1972, image of that scene is N34-33; E55-15. False-color diazo composites of MSS bands 4 (yellow), 5 (red), and 7 (blue) were prepared from positives of ERTS-1 images taken of the Great Kavir on September 2 and 20, 1972; December 19, 1972; February 11, 1973; March 1, 1973; and May 12, 1973 (figs. 16-21). The

route of the existing dry-season road was overlain on each diazo composite, and the seasonal hydrologic conditions along four critical segments of that route south of Moalleman were recorded (table 3). The hydrologic conditions at the surface of the Great Kavir are inferred from the ERTS-1 images on the basis of the author's field work in that area and along the dry-season road in October 1965 and September 1966, respectively.

The four critical road segments represent areas that are subject to soil saturation by water on even local flooding and thus require special engineering considerations. The road segment from kilometers 25 to 50 lies in the area underlain by Miocene bedrock (fig. 13). It is always moist along a narrow drainageway at kilometer 40 during the dry season, but this area becomes wet by mid-December. Dissolution of the local salt crust parallel to the drainageway suggests saturation of the surficial materials. By March, the surface in a slight depression is also wet at kilometer 32. The road from kilometers 25 to 50 can be aligned inexpensively to the west on good natural subgrade to avoid the two wet areas (fig. 21); culverts will be required along drainageways.

The segment from kilometer 60 to 63 lies in a depression within the area underlain by Miocene bedrock (fig. 13). It is always moist at kilometer 62 during the dry season and becomes moister by mid-December. This segment is wet by mid-May and a bridge or raised roadbed would be required at kilometer 62 (fig. 21).

The segment from kilometers 90 to 100 lies in an area that is occupied principally by salt crusts (fig. 13) which undergo significant changes in their surface conditions during the seasons. Salt crusts are dry during September but become moist by mid-December with some dissolution.

By early February, both soil and salt crusts are wet with continuing dissolution of the salt. Standing water is present by March 1, and its areal extent has increased by mid-May. This segment is the most difficult and would require both a raised roadbed and a bridge. Although an alignment to the east would avoid the wettest areas, the costs of engineering for the poor subgrade over the increased length of the road (up to 30 km) would be prohibitive (fig. 21).

The segment from kilometers 110 to 116, which lies within the area underlain by Miocene bedrock, is always moist at kilometer 113 during the dry season, and becomes moister by mid-December. By March 1, the surface is wet at kilometer 113 and this condition continues into May. This area can be avoided by a short alignment to the west (fig. 21).

The use of ERTS-1 images provides a method for examining areas that are seasonally inaccessible in order to determine hydrologic changes that affect soil conditions and thus their engineering properties. There must be some knowledge of actual ground conditions in order to correctly interpret the ERTS-1 images, and the eventual determination of the location of any engineering project such as a road alignment should be based on a longer record of observation and on-site investigation.

### Zagros Mountains Watershed

The Zagros Mountains Watershed (fig. 2) contains the Shiraz and Neriz Playas. Shiraz Playa is entirely within the folded belt of the Zagros, and Neriz Playa lies along the Zagros thrust zone.

Mesozoic limestones are the principal rock along the northeastern divide of the watershed; Eocene shales and limestones form the southwestern

divide. Small outcrops of Miocene rock adjacent to Shiraz Playa probably contain mostly shales or saliferous materials and some evaporites. The Bakhtiary gravels of mid-Pliocene age occur in scattered outcrops throughout the region.

### Neriz Playa

Neriz Playa has a high northern divide with altitudes of approximately 4,000 m. The southwestern divide (dashed line, fig. 2) is considerably lower with summits averaging approximately 2,600 m. The lowest pass lies along this divide at an altitude of 1,628 m, only 70 m above the playa surface. The annual precipitation decreases southeastward from 500 mm in the high mountains along the northwest divide to 191 mm at Neriz. The other divides generally receive from 200 to 300 mm of precipitation annually.

The streams from the higher northern divide of the watershed flow southeastward into the Rud-E-Kor (fig. 22) which empties into the Neriz Playa. The lower course of the principal channel of the Rud-E-Kor passes through an extensive delta deposit, the surface of which is 2 to 3 m above the adjacent playa. The channel was dry on August 12, 1967, except for a few scattered, brackish pools. Numerous smaller streams around the playa dry up by early summer but there are several spring-fed ponds which are a source of fresh water. These ponds generally occur at the base of a limestone knob or cliff and commonly contain small fish.

Neriz Playa was occupied by a doughnut-shaped Pleistocene lake whose surface was 3 m above the present playa at its maximum extent. Its former position is now marked by conspicuous beaches. Recent fan activity

has locally removed segments of these beaches, but their generally extensive distribution suggests that runoff in this part of the basin has been negligible. There are now two intermittent lakes at Neriz Playa that are separated at their western ends by the delta of the Rud-E-Kor. The northern lake is smaller, less well defined and is more apt to be obscured by clouds; it has not been analyzed in this study.

During June, 1956 (aerial photo date), the lakes extended over most of the salt crust. Bobek (1963, p. 406), who visited the playa at that time, reported that the southern lake, Lake Bakhtegan, was only one meter deep. In late August, 1965 the lakes occupied a smaller area, with more salt crust visible at their eastern margins. However, on August 10, 1967, the lakes had practically disappeared except for small areas adjacent to springs. Small woody plants near the shore of Lake Bakhtegan had recent vegetable debris in their branches, up to a height of one meter above the floor of the playa. Considering the low gradient of the surface towards the center of the playa, the maximum depth of the lake may have been 2 m within recent time.

The salt crust at Neriz Playa is extensive but poorly developed due to annual inundation by fresh water. The salt polygons are irregular with diameters of 130 to 150 cm. The raised edges are from 2 to 8 cm in height and fresh salt indicates continuing movement of capillary water during the dry season.

A pit illustrated in figure 23 was excavated on October 20, 1965. That year was considerably wetter than 1967; however, water was only encountered in the pit at a depth of 40 cm although the materials were moist throughout the section. The thinness of the salt crust (one

centimeter) and the absence of any other similar crusts in the section suggest that the crust is entirely dissolved during each spring flooding and redeposited during the dry season after evaporation of the briny lake.

In this report, the southern lake (Lake Bakhtegan) and its immediate playa area (797 km<sup>2</sup>) are analyzed. The area occupied by the Pleistocene lake was 1,915 km<sup>2</sup>.

### Shiraz Playa

The basin/playa ratio for Shiraz Playa (playa area is 247 km<sup>2</sup>) is 14.8 compared to 13.8 for Neriz Playa (considering the entire playa area of 1,915 km<sup>2</sup>). Note that Shiraz and Neriz Playas occupy separate basins within a larger watershed (fig. 2). The similarity in basin/playa ratios expresses itself hydrologically in the occurrence of beaches around the margin of Shiraz Playa which mark the level of an ancient shallow lake. The beaches are generally well-preserved except near the villages, or locally where they are now being removed by active fans.

The intermittent lake, although quite shallow, fills the center of the valley bottom during the spring runoff period. In April 1967, near its maximum seasonal extent, the greatest measured depth of the lake was 50 cm (Huber, 1967). Around the margin of the west shore of the lake the salt is 12.5 cm thick, which is considerably thicker than the Neriz salt crust, and which suggests that the streams discharging into the lake have a much higher saline content.

Water analyses from the two lakes (Pendleton, written communication, February 1970) provided the following data:

Lake Shiraz (ppm)	Lake Bakhtegan (ppm)
339,040 Mg	8,360 Mg
5,200 Na	125 Na
5,320 Cl	122 Cl

In the past, the larger proportion of lake area at Shiraz Playa has been considered to be due in part to its greater salinity, which reduces losses by evaporation (Harbeck, 1955, p. 1). Lake Shiraz contracts considerably during the summer, more in some years than in others, but in late October 1965 there was still a considerable body of water occupying the playa.

The salt crust is generally smooth and less than 2 cm thick, but in the central sector along the west shore where it attains a thickness of 12.5 cm, the salt is collected at the lake margin where it is purest (fig. 24), and sold locally for table use. Underlying the salt is a black briny mud which contains salt crystals. The mud is a well-sorted clayey-silt which has settled out of the lake, and in which the salt crystals have subsequently formed. The saline content of the black mud is extremely high (79 percent of the coarse fraction), which explains the diagenetic crystals.

Six beach strands are preserved in many areas along the northeastern shore of the playa. They are particularly well developed on a narrow promontory which is accessible by road from Shiraz.

It seems clear that the same or very similar climatic parameters that prevailed in the Neriz Basin during the late Pleistocene must have also existed in the Shiraz Basin. The absence of older and higher beaches does not preclude the existence of earlier Pleistocene lakes in this area.

It suggests that if these lakes did exist, they were also shallow and occupied the lower parts of the basins, which are now filled with sediments.

Recent fan activity, coupled with wide fluctuations in the lake levels, suggests that there has been an increase in runoff in the Zagros Mountains Watershed.

#### Analysis of the ERTS-1 Images of Shiraz and Neriz Playas

False-color composites of Shiraz and Neriz Playas (both playas appear in a single scene) were prepared from the ERTS-1 MSS positives of seven scenes (figs. 22, 25, 26). These are identified in table 4, which summarizes the lacustrine fluctuations in the playas from September 2, 1972, to August 28, 1973. These data were obtained by measuring the areas of the playas and of the lakes in each scene (fig. 27).

On September 2, 1972 (fig. 25), Lake Shiraz occupied 73 percent of the playa area and had an estimated average depth and volume of 0.2 m and  $36 \times 10^6$  m<sup>3</sup>, respectively (fig. 28). The southern lake at Neriz Playa occupied 23 percent of its immediate playa area and had an estimated average depth and volume of 0.5 m and  $93 \times 10^6$  m<sup>3</sup>, respectively. Water depths were generally uniformly distributed at Lake Shiraz, but at the Neriz lake, the deepest water was near its source in the western part of the playa. Receding waterlines are conspicuous as concentric zones in the thin salt crust of the playas.

By September 20, 1972 (fig. 25), Lake Shiraz had contracted to 66 percent of the playa area and had an estimated average depth and volume of 0.1 m and  $16 \times 10^6$  m<sup>3</sup>, respectively. The lake at Neriz



contracted to 21 percent of the playa area and had an estimated average depth and volume of 0.4 m and  $68 \times 10^6 \text{ m}^3$ , respectively. Except for a deep pool near the west shore of Lake Shiraz, water depths were uniformly distributed. The deepest water in the Neriz lake was in the western part of the playa; the long, narrow central area of the lake had very shallow water. This period at the end of the long, hot summer, during which rain is generally absent (fig. 28) and evaporation rates are highest, has the lowest ground water levels of the year.

Lake Shiraz reoccupied 73 percent of the playa area and had an estimated average depth and volume of 0.2 m and  $36 \times 10^6 \text{ m}^3$ , respectively, by December 19, 1972 (figs. 25, 28). The lake at Neriz expanded to 53 percent of its playa area and had an estimated average depth and volume of 0.7 m and  $301 \times 10^6 \text{ m}^3$ , respectively (figs. 27, 28). The deepest parts of both lakes were adjacent to their sources at the western ends of their playas. The greater rate of increase in the size of the Neriz lake relative to Lake Shiraz was due to its larger sources of ground water recharge during November and December (fig. 28).

By March 1, 1973 (fig. 26), Lake Shiraz occupied 94 percent of its playa area and had an estimated average depth and volume of 0.4 m and  $94 \times 10^6 \text{ m}^3$ , respectively. The lake at Neriz expanded to 99 percent of its playa area and had an estimated average depth and volume of 1.0 m and  $794 \times 10^6 \text{ m}^3$ , respectively. It seems reasonable to assume that some of the precipitation falling in the highest altitudes of the narrower Shiraz Basin would remain as snow, while most of the precipitation falling in the lower, broader valley of the Neriz Basin would be rain that quickly moved toward the playa. These considerations combined with the period

of the annual precipitation maximum and evaporation minimum could explain why the lake at Neriz appeared to reach its maximum extent ahead of Lake Shiraz.

Lake Shiraz occupied 97 percent of its playa area on March 19, 1973 (fig. 26), and had an estimated average depth and volume of 0.4 m and  $96 \times 10^6$  m<sup>3</sup>, respectively. The lake at Neriz contracted slightly to 85 percent of its playa area and had an estimated average depth and volume of 0.9 m and  $614 \times 10^6$  m<sup>3</sup>, respectively. The apparent maximum extent of Lake Shiraz is assumed to follow closely the period of maximum snowmelt (see above and fig. 28). The contraction of the lake at Neriz was probably due to drainage diversions from the two dams along the Rud-E-Kor.

By May 12, 1973 (figs. 22, 26), Lake Shiraz contracted to 86 percent of its playa area and had an estimated average depth and volume of 0.3 m and  $64 \times 10^6$  m<sup>3</sup>, respectively. The lake at Neriz expanded slightly to 90 percent of its playa area and had an estimated average depth and volume of 1.0 m and  $722 \times 10^6$  m<sup>3</sup>, respectively. The expansion of the Neriz lake suggests that the upstream dams were filled (note the reservoir along the Rud-E-Kor, north of Lake Shiraz, fig. 22) and that the large ground water sources were recharging the lake. This argument seems to be supported by the fact that the period of precipitation had ended and that temperature and evaporation had significantly increased (fig. 28). Lake Shiraz, unlike the lake at Neriz, has considerably less ground water storage and responds principally to current runoff.

On August 28, 1973 (figs. 26, 27), Lake Shiraz had contracted to one percent of its playa area and had an estimated average depth and volume of 0.3 m and  $0.9 \times 10^6$  m<sup>3</sup>, respectively. The lake at Neriz contracted

to 5 percent of its playa area and had an estimated average depth and volume of 0.5 m and  $19 \times 10^6$  m<sup>3</sup>, respectively. It is significant to observe the extreme variation of these lakes within a single year. Note that almost one full year after September 2, 1972 (fig. 25), Lake Shiraz had almost disappeared, and the lake at Neriz was reduced to one small lake and two separate ponds (figs. 26, 27). This extreme variation is due primarily to the marginal climatic equilibrium of these lakes, the delicate balance between precipitation and evaporation. The current lack of complete synchronicity between the lakes in the periods of minimum and maximum lake fluctuation is accentuated by man's intervention in the hydrologic cycle of these lakes by his increased water diversions through dams and pumped wells.

#### Potential for Economic Development

From February through May 1973 there were at least  $600 \times 10^6$  m<sup>3</sup> of water available from the lake at Neriz (fig. 28). This figure obviously may vary annually with the climate and with the magnitude of the drainage diversions. This region is important agriculturally, and more recently it has become the site for industrial development including a large oil refinery. Consequently, there is need for the large amount of water that is lost to evaporation each year. The evaporation is facilitated by a large body of very shallow water. Larger, deeper reservoirs are required to store the water during the long dry summer. Consideration should also be given to the ecological and local economic effects of further water withdrawals from the lake. The larger villages along the southern shore of the lake have qanats for fresh water, but use pumped wells to augment

irrigation. If the lake disappears, there will be local climatic effects such as accentuation of the aridity of the area and changes in the plant and animal communities. These hydrologic and biologic changes may be undesirable and irreversible, and should be carefully reviewed before any additional water is removed.

Although the salt crust at the Neriz Playa is thin, there may be buried crusts which are thicker as well as brines which have salts of economic value. The general accessibility of the playa and its deposits argue for a systematic investigation of its resource potential.

Lake Shiraz had a relatively negligible water supply from February through May 1973 (at least  $50 \times 10^6$  m<sup>3</sup> of water, fig. 28). Some of this water could no doubt be diverted for agricultural or industrial use, but the withdrawal would seriously affect the discharge from the several pumped wells in the vicinity. The amount of water is marginal and may not justify any significant expenditures of money for diversions and storage. Salt from the west shore area is currently used for human consumption and this use could no doubt be expanded.

#### CONCLUSIONS

ERTS-1 generated images constitute an important tool for the evaluation of some Iranian Playas as sites for economic and engineering development. Even when used alone and interpreted far from the image area, an experienced earth scientist can make many sound inferences concerning the hydrology, morphology, and to some extent the gross pedology of the playas.

The reliability of the interpretation is significantly improved if the interpreter is familiar with ground conditions in the image area.

The degree of detail and the scope of the interpretation are even further improved through the application of computer-enhanced techniques to the ERTS-1 images.

Iran in general and its playas in particular lend themselves to generally unimpaired observation during most of the year. An arid environment with no vegetation and almost no macrorelief provides a flat target area in which minor hydrologic changes are immediately visible, particularly in band 7. These changes, when considered with respect to the known composition of the surficial materials, permit a generally valid evaluation of the bearing strengths of the sediments at the time the image is made.

As detailed and illustrated in this study of the playa lakes at Qom, Shiraz, and Neriz, the repetitive coverage of ERTS-1 is ideally suited to provide a seasonal record and an annual inventory of the hydrologic balance of water bodies that are otherwise not measured or would be difficult and expensive to measure by other means. Only a modest amount of ground control (water depth measurements at maximum and intermediate stages) would increase the reliability of water balance calculations significantly.

Because of their generally uniform appearance, playa surficial materials are usually sampled randomly, in the absence of any conspicuous differences in textures, moisture, relief, or color. The use of a computer-enhanced image permits the earth scientist to concentrate on specific areas of discrete image color changes which must reflect differences in hydrology, composition, and relief, or some subtle combination of all three. Once some equivalence has been achieved between the computer-enhanced image

signature and the actual surficial conditions, computers could be programmed to receive images and respond to materials, textures, moisture, and bearing strengths.

The ERTS-1 images may be sufficient for many future sophisticated uses, or they may require the additional use of one or more remote sensing tools to further investigate the resources of our planet and to monitor environmental conditions and hazards.

## REFERENCES

- Billingsley, F. C., Goetz, A. F. H., and Lindsley, J. N., 1970, Color differentiation by computer image processing: *Photog. Sci. and Engineering*, v. 14, no. 1, p. 28-35.
- Bobek, H., 1963, Nature and implications of Quaternary climatic changes in Iran: *Symposium on Changes of Climate, Rome, Oct. 1961, UNESCO-WMO*, p. 403-413.
- Gansser, A., 1955, New aspects of the geology in central Iran in *World Petroleum Congress, 4th Rome, 1955, Proc., sec. I, Geology Geophysics*, p. 279-300.
- Harbeck, Jr., G. E., 1955, The effect of salinity on evaporation: *U.S. Geol. Survey Prof. Paper 272-A*, 6 p.
- Huber, H., 1960, The Quaternary deposits of the Darya-i-Namak, central Iran: *Iran Oil Co., Geol. Note 51, Appendix*, 4 p., *Stratigraphic Section*.
- \_\_\_\_\_ 1967, Geological map of Maharlu Salt Lake southwest of Shiraz, Fars Province: *National Iranian Oil Co., Geol. Note 157, enclosure 2*.
- Issar, A., 1969, The ground water provinces of Iran: *Internat. Assoc. Sci. Hydrol. Bull.*, v. 14, no. 1, p. 87-99.
- Krinsley, D. B., 1968, Geomorphology of three kavirs in northern Iran in *Playa surface morphology: miscellaneous investigations: Cambridge Research Lab. Environmental Research Paper no. 283, U.S. Geological Survey for U.S. Air Force*, p. 105-130.
- \_\_\_\_\_ 1969, Caractères morpho-climatiques des kavirs d'Iran (The morpho-climatic aspects of Iranian kavirs): *Resumés des Communications, VIII Congrès INQUA, Paris*, p. 33.

Krinsley, D. B., 1970, A geomorphological and paleoclimatological study of the playas of Iran: U.S. Geol. Survey Interagency Rept. Military-1, 329 p., 4 plates, 155 figs., 17 tables.

\_\_\_\_\_ 1972a, Dynamic processes in the morphogenesis of salt crusts within the Great Kavir; north-central Iran, in Internat. Geol. Cong., 24th, Montreal, Proc., sec. 12, p. 167-174.

\_\_\_\_\_ 1972b, The paleoclimatic significance of the Iranian Playas, in Zinderen Bakker, E. M. Van, ed., Palaeoecology of Africa: Cape Town, A. A. Balkema, v. 6, p. 114-120.

National Iranian Oil Company, 1959, Geological Map of Iran (1:2,500,000) with explanatory notes, Zurich, Orell Fussli.

Oberlander, T., 1968, Hydrography, in Fisher, W. B., The Cambridge History of Iran, The Land of Iran: Cambridge Univ. Press, v. 1, p. 264-279.